

## CONSTRAINTS ON PRIMORDIAL NONGAUSSIANTY FROM THE HIGH-REDSHIFT CLUSTER MS1054-03

JEFFREY A. WILICK<sup>1</sup>

Department of Physics, Stanford University, Stanford, CA 94305-4060  
 E-mail: jeffw@perseus.stanford.edu

*Submitted to the Astrophysical Journal*

### ABSTRACT

The implications of the massive, X-ray selected cluster of galaxies MS1054-03 at  $z = 0.83$  are discussed in light of the hypothesis that the primordial density fluctuations may be nongaussian. We generalize the Press-Schechter (PS) formalism to the nongaussian case, and calculate the likelihood that a cluster as massive as MS1054 would have been found in the Einstein Medium Sensitivity Survey (EMSS). A flat universe ( $\Omega_M + \Omega_\Lambda = 1$ ) is assumed and the mass fluctuation amplitude is normalized to the present-day cluster abundance. The probability of finding an MS1054-like cluster then depends only on  $\Omega_M$  and the extent of primordial nongaussianity. We quantify the latter by adopting a specific functional form for the PDF, denoted  $\psi_\lambda$ , which tends to Gaussianity for  $\lambda \gg 1$  but is significantly nongaussian for  $\lambda \lesssim 10$ , and show how  $\lambda$  is related to the more familiar statistic  $T$ , the probability of  $\geq 3\sigma$  fluctuations for a given PDF relative to a Gaussian. Special attention is given to a careful calculation of the virial mass of MS1054 from the available X-ray temperature, galaxy velocity, and weak lensing data.

We find that Gaussian initial density fluctuations are consistent with the data on MS1054 only if  $\Omega_M \lesssim 0.2$ . For  $\Omega_M \geq 0.25$  a significant degree of nongaussianity is required, unless the mass of MS1054 has been substantially overestimated by X-ray and weak lensing data. The required amount of nongaussianity is a rapidly increasing function of  $\Omega_M$  for  $0.25 \leq \Omega_M \leq 0.45$ , with  $\lambda \leq 1$  ( $T \gtrsim 7$ ) at the upper end of this range. For a fiducial  $\Omega_M = 0.3$ ,  $\Omega_\Lambda = 0.7$  universe, favored by several lines of evidence (Wang *et al.* 1999), we obtain an upper limit  $\lambda \leq 10$ , corresponding to a  $T \geq 3$ . This finding is consistent with the conclusions of Koyama, Soda, & Taruya (1999), who applied the generalized PS formalism to low ( $z \lesssim 0.1$ ) and intermediate ( $z \lesssim 0.6$ ) redshift cluster data sets.

### 1. INTRODUCTION

A working hypothesis in most approaches to cosmological structure formation is that the density fluctuation field  $\delta(\mathbf{x})$  is Gaussian at early times. This assumption follows naturally from the idea that the primordial fluctuations may be described as superpositions of statistically independent Fourier modes,

$$\delta(\mathbf{x}) = \sum \delta_{\mathbf{k}} e^{i\mathbf{k}\cdot\mathbf{x}}. \quad (1)$$

Such modes are generic predictions of inflation, in which quantum fluctuations are exponentially enlarged to become the classical density fluctuations. Whatever the form of the power spectrum  $P(k) = |\delta_{\mathbf{k}}|^2$ , the independence of the Fourier modes guarantees, by the central limit theorem, that the real-space density fluctuations are Gaussian.

Although the Gaussian hypothesis is well-motivated, several lines of argument suggest that it merits further scrutiny. On the theoretical side, Peebles (1999a,b) has presented a model in which nongaussianity emerges naturally in a modified inflationary scenario. The key ingredient is that the scalar field which drives inflation,  $\psi$ , couples quadratically to a massive scalar field  $\phi$  which, at the end of inflation, produces the cold dark matter (CDM). The CDM density field is then given by  $\rho_{CDM}(\mathbf{x}) = \mu^2 \phi^2(\mathbf{x})/2$ , where  $\phi(\mathbf{x})$  is a Gaussian random field. The fluctuations in the CDM component,  $\delta(\mathbf{x}) \propto \rho_{CDM}(\mathbf{x}) - \langle \rho_{CDM} \rangle$ , are thus distributed like a  $\chi^2$  function shifted to have vanishing mean. Such a distribution is strongly nongaussian,

with significant skew and excess kurtosis. (Other inflationary models which lead to nongaussian density fluctuations have recently been described by Salopek [1999] and by Martin, Riazuelo, & Sakellariadou [1999].)

Peebles' model has been extended by White (1998) and by Koyama, Soda, & Taruya (1999), who have considered models in which the CDM is produced by a finite number,  $m$ , of quadratically coupled fields. The resulting density fluctuations would then have a  $\chi_m^2$  distribution (again, shifted to have mean zero), which approaches Gaussianity in the limit of large  $m$ . In this way one can generate primordial fluctuations with any desired amount of nongaussianity. However, the required number of quadratically coupled fields must be quite large ( $\gtrsim 100$ ) if the wanted amount of nongaussianity is small. Such a large number of inflationary fields arguably makes this model contrived.

On the observational side, hints of nongaussianity have emerged, first, from Cosmic Background Radiation (CBR) anisotropy maps. Ferreira *et al.* (1998, 1999; see also Magueijo 1999) analyzed the full-sky COBE-DMR maps (Bennett *et al.* 1996), finding evidence of nongaussianity on large ( $\gtrsim 10^\circ$ ) angular scales using a statistic known as the normalized bispectrum estimator. This finding was confirmed by two independent analyses using alternative statistical techniques (Novikov, Feldman, & Shandarin, 1998; Pando, Valls-Gabaud, & Fang, 1998). These studies appear to rule out Gaussianity of the CBR anisotropies at about the 95% confidence level. A curious feature of these COBE-DMR results is that the nongaussian signal

<sup>1</sup>Cottrell Scholar of Research Corporation

goes away if the north galactic cap is excluded from the analysis; this is a surprising property, one that argues for caution in ascribing reality to these findings (see Bromley & Tegmark 1999 for a detailed treatment of this issue). In an unrelated study of CBR anisotropy detections on degree scales, Gaztañaga, Fosalba, & Elizalde (1998) found evidence for nongaussianity based on the large variance among the reported anisotropy amplitudes. This finding, like that of Ferreira *et al.*, should be considered preliminary, as it is based on an intercomparison of very different data sets and is strongly dependent on the accuracy of the reported errors. Nonetheless, these results from CBR anisotropy data call into question the hypothesis of primordial gaussianity.

The second line of observational evidence comes from the abundance and clustering of rich clusters of galaxies. As the most massive virialized systems in the universe, rich clusters are diagnostic of the background cosmological parameters in a number of ways (cf. Bahcall 1999 for a recent review). In particular, their number density and correlation length, as a function of mass and redshift, can be predicted from the Press-Schechter (1974, hereafter PS) formalism, summarized in § 2 below. The original PS formalism assumes primordial Gaussianity, but this assumption is readily relaxed, leading to a generalized PS approach (§ 2.3). Robinson, Gawiser, & Silk (1998) applied the generalized PS formalism to low-redshift ( $z \lesssim 0.1$ ) cluster abundance and correlation data. They found the data to be consistent with the Gaussian hypothesis in an  $\Omega_M = 1$  universe.<sup>2</sup> For lower values of the density parameter, however, Robinson *et al.* found that a substantial degree of primordial nongaussianity is required to reconcile the number density of massive clusters with their observed correlation length. Koyama, Soda, & Taruya (1999) further narrowed these constraints by applying the generalized PS formalism to intermediate-redshift ( $z \simeq 0.5$ – $0.6$ ) cluster abundance data, as well as to the low redshift data sets studied by Robinson *et al.* They found that  $\Omega_M > 0.5$  was ruled out by the combined data sets regardless of the nature of the initial density fluctuations, and that Gaussian fluctuations were ruled out for  $\Omega_M \leq 0.5$ . We defer a fuller discussion of their results to the final section of this paper, after introducing the necessary terminology in § 3.

The studies cited above provide evidence that the hypothesis of Gaussian density fluctuations is violated at some level. The purpose of this paper is to extend the analyses of Robinson *et al.* (1998) and Koyama *et al.* (1999) by applying the generalized PS approach to a single high-redshift cluster, MS1054-03, which at  $z = 0.83$  is one of the highest redshift clusters known. It is, moreover, the most extensively studied of the known high-redshift clusters; its mass has been accurately estimated by the techniques of weak gravitational lensing (Luppino & Kaiser 1997), X-ray temperature analysis (Donahue *et al.* 1998), and galaxy velocity dispersion (Tran *et al.* 1999). These studies all found that MS1054 is an unusually massive cluster, with a virial mass  $\gtrsim 10^{15} h^{-1} M_\odot$ . Its high redshift, large and accurately determined mass, and its having been selected from the Einstein Medium Sensitivity Survey (Henry *et al.* 1992; EMSS), whose selection criteria

are very well understood, combine to make MS1054 especially well suited for the present study. A previous analysis of MS1054 (Bahcall & Fan 1998) noted these features, and derived important cosmological constraints, but did so under the assumption of primordial Gaussianity. We will extend their results by including nongaussianity as an additional degree of freedom.

This paper is also meant to serve two additional purposes. First, we will introduce (§ 3) a new mathematical description of nongaussian density fluctuations, in the form of a probability distribution function (PDF) we refer to as the  $\psi_\lambda$ -distribution. We will discuss the relationship between the  $\psi_\lambda$  and  $\chi^2_m$  distributions, and argue that the former is preferable to the extent that a fully generic, model-independent parameterization of nongaussianity is desired. Second, we will present (§ 4) a detailed discussion of the proper determination of cluster virial masses from X-ray temperature, galaxy velocity dispersion, and weak lensing data sets, and apply the results to MS1054. This discussion will, it is hoped, be useful in clarifying the ways in which virial masses are dependent on cosmological parameters and, more subtly, on cluster mass models, and thus inform future studies based on larger data sets.

The outline of this paper is as follows. In § 2, we describe the Gaussian and generalized PS formalisms. In § 3, we introduce the  $\psi_\lambda$  distribution. In § 4 we discuss the determination of cluster virial masses. In § 5 we use published data to estimate the virial mass of MS1054. In § 6 we apply the generalized PS formalism to MS1054 and derive constraints on nongaussianity as a function of  $\Omega_M$ . Finally, in § 7, we further discuss and summarize the main results of the paper.

## 2. THE PRESS-SCHECHTER FORMALISM AND ITS EXTENSION TO THE NONGAUSSIAN CASE

Under the assumption of primordial Gaussianity, the PS formula for the comoving number density of virialized objects of mass  $M$  is

$$n(M, z) = \sqrt{\frac{2}{\pi}} \frac{\bar{\rho}}{M^2} \frac{\delta_c(z)}{\sigma_M} \left| \frac{d \ln \sigma_M}{d \ln M} \right| e^{-\delta_c(z)^2 / 2\sigma_M^2}, \quad (2)$$

where  $\sigma_M$  is the rms mass fluctuation on a mass scale  $M$ ,  $\bar{\rho} \equiv \Omega_M \rho_{crit}$  is the comoving mean mass density, and  $\delta_c(z)$  is the critical density for collapse at redshift  $z$ . Because  $\sigma_M$  is by definition the rms density fluctuation linearly extrapolated to the present,  $\delta_c(z)$  is similarly normalized to the present,

$$\delta_c(z; \Omega_M, \Omega_\Lambda) = \delta_0(z) \frac{D(z=0; \Omega_M, \Omega_\Lambda)}{D(z; \Omega_M, \Omega_\Lambda)}. \quad (3)$$

The linear fluctuation growth factor is given by

$$D(z; \Omega_M, \Omega_\Lambda) = \frac{5}{2} \Omega_M E(z) \int_z^\infty \frac{1+z'}{E(z')^3} dz', \quad (4)$$

where  $E(z) = \sqrt{\Omega_M(1+z)^3 + \Omega_R(1+z)^2 + \Omega_\Lambda}$ ,  $\Omega_M + \Omega_R + \Omega_\Lambda = 1$ , and we are following Peebles' (1993) notation. Throughout this paper we assume a flat universe,  $\Omega_R = 0$ .

<sup>2</sup>Here and throughout this paper, the present value of the mass density parameter is denoted  $\Omega_M$ , while the density parameter associated with a cosmological constant  $\Lambda$  (or, equivalently, vacuum energy density) is denoted  $\Omega_\Lambda$ . The Hubble constant is written as  $H_0 = 100 h \text{ km s}^{-1} \text{ Mpc}^{-1}$ .

The quantity  $\delta_0(z)$  in equation 3 is the famous factor  $3(12\pi)^{2/3}/20 = 1.686$  for an Einstein de-Sitter universe. It has a weak dependence on cosmological parameters and redshift. In this paper, we use the forms of  $\delta_0(z)$  derived by Kitayama & Suto (1996).

### 2.1. Calculation of $\sigma_M$

The rms mass fluctuation  $\sigma_M$  in equation 2 is computed from the linear power spectrum  $P(k)$  as follows:

$$\sigma_M^2 = \int_0^\infty \frac{dk}{k} \Delta^2(k) W^2(kR), \quad (5)$$

where  $\Delta^2(k) \equiv k^3 P(k)/2\pi^2$  is the mass variance per logarithmic wavenumber interval,  $W(kR)$  is the Fourier transform of the window function defining the mass scale  $M$ , which we take to be the usual top-hat, and  $R$  is the radius of a sphere which contains mass  $M$  in an unperturbed universe. In this paper we assume a CDM-dominated universe, in which the power spectrum is well-approximated by

$$\Delta^2(k) = \delta_H^2(\Omega_M, \Omega_\Lambda) \left( \frac{ck}{H_0} \right)^{3+n} T^2(k/\Gamma) \quad (6)$$

(Bunn & White 1997), where  $\delta_H$  is the rms overdensity at horizon-crossing,  $n$  is the primordial spectral index, and  $T(q)$  is the CDM transfer function, for which we adopt the analytic approximation of Bardeen *et al.* (1986). The parameter  $\Gamma$  determines the position of the power-spectrum ‘‘turnover’’ in  $k$ -space. For CDM it is given by  $\Gamma \approx \Omega_M h$ . For the calculations of this paper, the precise value of  $\Gamma$  is relatively unimportant, and we adopt the value  $\Gamma = 0.20$ , consistent with observations of large-scale structure data (e.g., Liddle *et al.* 1996) and with the CDM expectation for reasonable values of the cosmological parameters. We also assume  $n = 1$ , consistent with estimates derived from the large-scale CBR anisotropies observed by COBE (Gorski *et al.* 1996). Changing our adopted values of  $\Gamma$  and  $n$  by  $\lesssim 20\%$ , roughly their allowed ranges, would have little effect on the main conclusions of this paper.

### 2.2. Conversion to useful units

To make practical calculations, we reexpress the PS formula in terms of suitably scaled variables. We first define a dimensionless mass  $m$  by

$$M = \frac{4\pi}{3} r_8^3 \rho_{crit} m = 5.95 \times 10^{14} m h^{-1} M_\odot, \quad (7)$$

where  $r_8 \equiv 8 h^{-1}$  Mpc and  $\rho_{crit} = 3H_0^2/8\pi G$  is the critical density. For rich clusters,  $m$  is of order unity. Let  $n(m)dm$  be the comoving number density of clusters with dimensionless masses in the range  $(m, m + dm)$ . Then

$$n(m, z) = n(M, z) \frac{dM}{dm} = \sqrt{\frac{2}{\pi}} \frac{3\Omega_M}{4\pi r_8^3 m^2} \frac{\delta_c(z)}{\sigma_M} \left| \frac{d \ln \sigma_M}{d \ln M} \right| e^{-\delta_c(z)^2/2\sigma_M^2}, \quad (8)$$

where we have substituted the definition of  $m$  into equation 1. Furthermore, as noted above, we compute  $\sigma_M$  not

as a function of mass but of a length scale  $R_m$  defined by  $M = \frac{4}{3}\pi R_m^3 \Omega_M \rho_{crit}$ , or equivalently,

$$R_m = r_8 \left( \frac{m}{\Omega_M} \right)^{1/3}. \quad (9)$$

Thus,  $d \ln \sigma_M / d \ln M = 1/3 \times d \ln \sigma_M / d \ln R$ . Substituting this into equation 8 and evaluating numerical factors yields

$$n(m, z) = n_0 \frac{\Omega_M}{m^2} \left| \frac{d \ln \sigma_M}{d \ln R} \right|_{R_m} \nu_m \phi(\nu_m), \quad (10)$$

where  $n_0 = 3.11 \times 10^{-4} (h^{-1} \text{Mpc})^{-3}$ ,  $\phi(x)$  is a Gaussian of zero mean and unit variance, and  $\nu_m(z) \equiv \delta_c(z; \Omega_M) / \sigma_M(R_m)$ . Equation 10 gives the comoving number density per unit dimensionless mass; note that most of the  $\Omega_M$ -dependence of this expression resides in the factor  $\nu_m$ , not in the  $\Omega_M$  out in front. Finally, the directly observed quantity is  $N(\geq m, z)$ , the comoving number density of all clusters of mass  $\geq m$  at redshift  $z$ , given by

$$N(\geq m, z) = n_0 \Omega_M \int_m^\infty \frac{dm'}{m'^2} \left| \frac{d \ln \sigma_M}{d \ln R} \right|_{R_{m'}} \nu_{m'} \phi(\nu_{m'}). \quad (11)$$

### 2.3. Extension to Nongaussian Fluctuations

The above formulae assumed a Gaussian PDF. We now relax this assumption, and assume only that the PDF,  $P(\delta|M)$ , is such that  $\langle \delta \rangle = 0$  and that  $\langle \delta^2 \rangle = \sigma_M^2$ . It is useful to express the PDF in terms of a dimensionless function  $\psi(x)$  as follows:

$$P(\delta|M) = \sigma_M^{-1} \psi \left( \frac{\delta}{\sigma_M} \right), \quad (12)$$

where  $\psi(x)$  satisfies the conditions  $\int \psi(x) dx = 1$ ,  $\int x \psi(x) dx = 0$ , and  $\int x^2 \psi(x) dx = 1$ .

If one now retraces the usual steps leading to the PS abundance formula, equation 2, but using the PDF given by equation 12 in place of the usual Gaussian, one arrives at the expression

$$n(M, z) = \frac{2f_\psi \bar{p}}{M^2} \frac{\delta_c(z)}{\sigma_M} \left| \frac{d \ln \sigma_M}{d \ln M} \right| \psi \left( \frac{\delta_c(z)}{\sigma_M} \right). \quad (13)$$

The quantity  $f_\psi$  is given by  $(2 \int_0^\infty \psi(x) dx)^{-1}$ ; it corrects for underdense regions that are incorporated into virialized structures according to the standard PS ansatz. Equation 13 is our generalization of the PS formalism for non-Gaussian density perturbations. Setting  $\psi(x)$  to a Gaussian yields equation 1, as may readily be verified. Adopting dimensionless mass units and repeating the steps of § 2.2, we obtain for  $N(\geq m, z)$  the result

$$N(\geq m, z) = f_\psi n_0 \Omega_M \int_m^\infty \frac{dm'}{m'^2} \left| \frac{d \ln \sigma_M}{d \ln R} \right|_{R_{m'}} \nu_{m'} \psi(\nu_{m'}), \quad (14)$$

where the meaning of  $n_0$  and  $\nu_m$  are the same as above. The difference between the standard and generalized PS abundance predictions thus consists simply in replacing the Gaussian PDF  $\phi$  by the function  $\psi$ , apart for the factor  $f_\psi$ , which as shown below is  $\sim 1$  for cases of interest.

## 3. DESCRIPTION OF NONGAUSSIANITY

We wish to consider non-Gaussian fluctuations generically, i.e., to construct a PDF meeting the above conditions but which is not tied to a particular model. Moreover, we want our distribution to contain a parameter which quantifies the degree of nongaussianity. As noted above, a possible choice is the  $\chi_m^2$  distribution, a generalization of the Peebles (1999a,b) model proposed by White (1998) and by Koyama *et al.* (1999). Here we suggest an alternative parameterization. Our reasons for doing so are twofold: first, the  $\chi_m^2$  distribution is associated with a particular physical model, whereas our preference is to avoid such association at this preliminary stage in our understanding of the primordial fluctuations; and second, the  $\chi_m^2$  model approaches gaussianity only in the limit of very large  $m$ , a fact which makes the physical interpretation difficult to sustain if the observationally required degree of nongaussianity is slight.

Our model is based on a modified form of the Poisson distribution. Consider, first, an integer random variable  $n$  that is Poisson-distributed with expectation value  $\lambda$ . The probability that  $n$  takes on a particular integer value  $m$  is

$$P(n = m) = \frac{\lambda^m}{m!} e^{-\lambda}. \quad (15)$$

The rms deviation of  $n$  is  $\sqrt{\lambda}$ . We now imagine that  $n$  is continuous rather than discrete, and define a related random variable  $x \equiv (n - \lambda)/\sqrt{\lambda}$ . The probability distribution of  $x$ , which we refer to as  $\psi_\lambda(x)$ , is a modified form of the Poisson distribution, but shifted and scaled so that it has mean zero and unit variance. We obtain an explicit representation of  $\psi_\lambda(x)$  by letting  $m = \sqrt{\lambda}x + \lambda$  in equation 15, and then multiplying by  $\sqrt{\lambda}$  to renormalize the distribution. In addition, the factorial function in the denominator, which is defined only for integer values of its argument, must be replaced by its appropriate generalization for continuous variables, the  $\Gamma$ -function. This yields

$$\psi_\lambda(x) = \frac{\lambda^{\sqrt{\lambda}x + \lambda + \frac{1}{2}} e^{-\lambda}}{\Gamma(\sqrt{\lambda}x + \lambda + 1)}. \quad (16)$$

This function is defined for  $x > -(\sqrt{\lambda} + 1/\sqrt{\lambda})$ . As we now show,  $\psi_\lambda(x)$  is a suitable representation of quantifiable, generic departures from Gaussianity.<sup>3</sup>

<sup>3</sup>We note that equation 16 does not guarantee that  $\psi_\lambda(x)$  will have the key properties we seek: normalization, vanishing mean, and unit variance. For small  $\lambda$ , the transition from integer to continuous arguments does not preserve these properties, which were inherent in the parent Poisson distribution. By direct integration we have found that departures from these properties are completely negligible for  $\lambda > 10$ . For  $\lambda < 10$ , we correct  $\psi_\lambda(x)$  using formulae derived by fitting the deviations from normalization, vanishing mean, and unit variance. However, these corrections are extremely small for the cases of interest, so that equation 16 is fully adequate for our purposes.

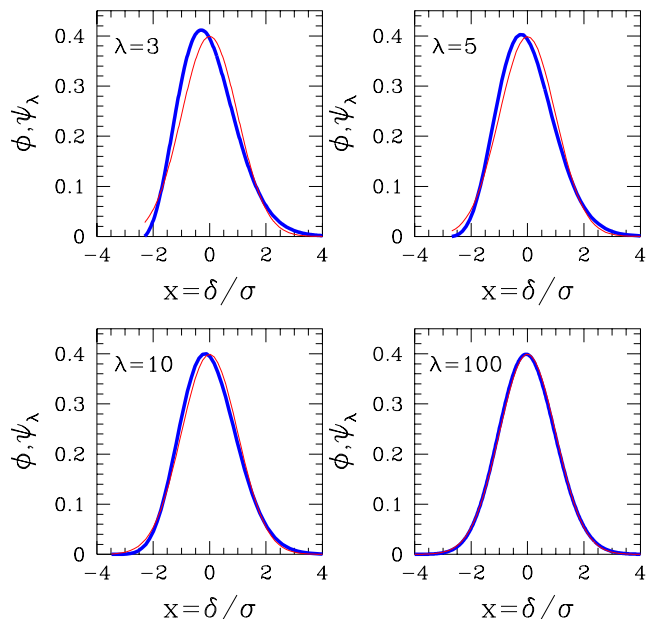


FIG. 1.— Comparison of a Gaussian,  $\phi$  (thin red curve) with the  $\psi_\lambda$  distribution (heavy blue curve), equation 16, for four values of the parameter  $\lambda$ . Note the progression of  $\psi_\lambda$  toward Gaussianity for  $\lambda \gg 1$ .

Figure 1 compares the  $\psi_\lambda$  distribution with a Gaussian for four values of the parameter  $\lambda$ . For  $\lambda = 3$ , the differences between the two are readily apparent; in particular, one sees the significant skewness of the  $\psi_\lambda$  distribution. For  $\lambda = 5$ , analogous differences can be seen, but they are noticeably smaller, and for  $\lambda = 10$  the differences are very small. For  $\lambda = 100$ , the  $\psi_\lambda$  is indistinguishable, on this plot, from a Gaussian.

The differences between  $\psi_\lambda$  and a Gaussian,  $\phi$ , become more apparent, even for  $\lambda \gtrsim 10$ , if we examine their behavior for large values of  $\delta/\sigma$ . This is shown in Figure 2 for the same four values of  $\lambda$  as in the previous figure. We see that for  $\lambda \lesssim 10$ ,  $\psi_\lambda(x)$  can exceed  $\phi(x)$  by 2–3 or more orders of magnitude for  $\delta/\sigma \gtrsim 4$ . As noted in § 2, this same factor enters directly into the PS-predicted cluster abundance. Thus, we expect that if the PDF is described by the  $\psi_\lambda$  distribution, massive clusters, representing rare peaks in the initial density field, will be far more abundant than they will in the Gaussian case, provided  $\lambda$  is not too large.

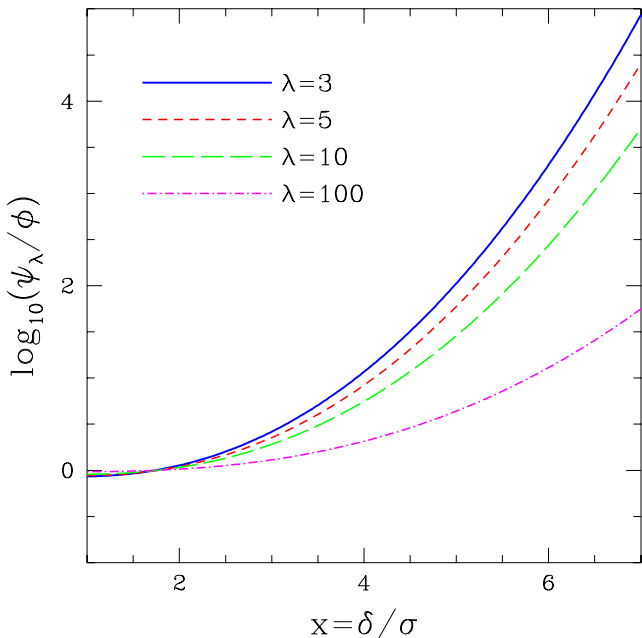


FIG. 2.— The ratio of  $\psi_\lambda$  to a Gaussian,  $\phi$ , plotted for values of the argument  $x \geq 1$ . The plotted ratio shows that “rare events,”  $\delta/\sigma \gtrsim 3$ , are considerably more likely if the distribution of overdensities is described by the  $\psi_\lambda$  function for  $\lambda \lesssim 10$ , than they are in the Gaussian case.

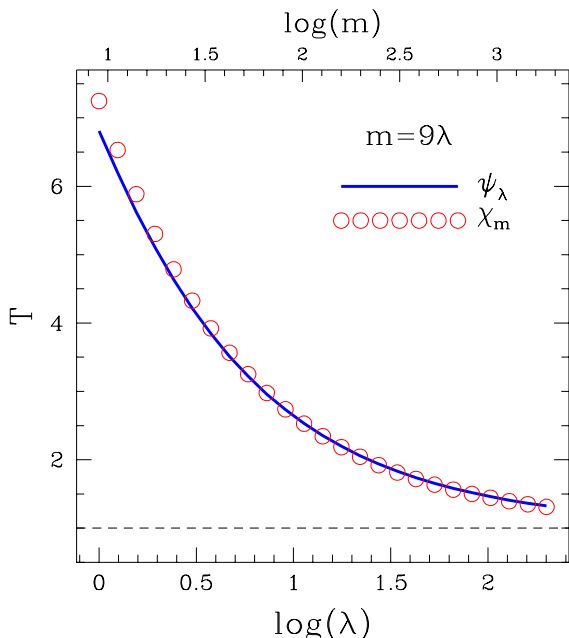


FIG. 3.— The T statistics of the  $\psi_\lambda$  (solid line) and  $\chi_m^2$  distributions (open circles) plotted versus their respective parameters,  $\lambda$  and  $m$ . The axes are scaled such that  $m = 9\lambda$ . The close agreement of the T statistics for the two distributions reveals their strong similarity in terms of the likelihood of rare ( $\gtrsim 3\sigma$ ) events, if one chooses  $m = 9\lambda$ .

The factor  $f_\psi$  that appears in equation 13 may be calculated numerically for the  $\psi_\lambda$  distribution. We have done so for  $2 \leq \lambda \leq 300$ . Within this range the numerical results are very well approximated by the expression

$$f_\psi(\lambda) = 1 + 0.149\lambda^{-0.528}. \quad (17)$$

Note that  $f_\psi$  differs from unity by less than 10% for  $\lambda \gtrsim 2$ .

### 3.1. Comparison with the $\chi_m^2$ distribution

The model introduced by White (1998) and by Koyama, Soda, & Taruya (1999) postulates that the CDM density field is given by

$$\rho_{CDM}(\mathbf{x}) = \frac{\mu}{2} \sum_{i=1}^m \phi_i^2(\mathbf{x}) \quad (18)$$

where the  $\phi_i(\mathbf{x})$  are statistically independent Gaussian fields. The overdensity  $\nu = \delta/\sigma$  in this model is distributed like a  $\chi^2$  variable with  $m$  degrees of freedom, shifted to have vanishing mean and unit variance. Explicitly,

$$P(\nu)d\nu = \frac{\left(1 + \sqrt{\frac{2}{m}}\nu\right)^{m/2-1}}{\left(\frac{2}{m}\right)^{(m-1)/2} \Gamma\left(\frac{m}{2}\right)} \exp\left(-\frac{m}{2} - \sqrt{\frac{m}{2}}\nu\right) d\nu, \quad (19)$$

a distribution we henceforth label  $\chi_m^2$ .

Koyama, Soda, & Taruya (1999) (see also Robinson, Gawiser, & Silk 1998) have advocated quantifying “rare event” nongaussianity in terms of a “T-statistic” defined by

$$T = \frac{\sqrt{2\pi} \int_3^\infty P(\nu)d\nu}{\int_3^\infty e^{-\nu^2/2} d\nu}, \quad (20)$$

the likelihood relative to Gaussian of  $3\sigma$  or rarer events. In terms of this statistic the relationship between the  $\psi_\lambda$  and  $\chi_m^2$  distributions becomes particularly clear. In Figure 3, the T statistics for the two distributions are plotted versus their respective parameters, with the axes scaled such that  $m = 9\lambda$ . With this scaling, the two distributions have T statistics which agree to within a few percent for all  $\lambda$ . This shows that in terms of the likelihood of rare events, the  $\psi_\lambda$  and  $\chi_m^2$  distributions are extremely similar for  $m = 9\lambda$ . It is also interesting to note that, despite the near-indistinguishability of  $\psi_\lambda$  from a Gaussian for  $\lambda \gtrsim 100$  (Figure 1), the two distributions approach the Gaussian value  $T = 1$  extremely slowly as  $\lambda \rightarrow \infty$ . Indeed, one requires  $m \simeq 200$  even to achieve  $T = 2$ , twice the Gaussian value. It is for this reason that the  $\chi_m^2$  model may not be suitable for describing mild Gaussianity—at least if one were to take its physical basis seriously—because the required number of primordial Gaussian fields is excessively large.

## 4. ON THE DETERMINATION OF CLUSTER VIRIAL MASSES

It is essential when applying PS abundance estimates that one use the rigorous definition of virial mass. Specifically, the PS formulae apply to the mass  $M_V$  interior to a radius  $r_V$  such that  $3M_V/4\pi r_V^3 = \Delta_V(z, \Omega_M, \Omega_\Lambda)\bar{\rho}(z)$ , where  $\Delta_V(z, \Omega_M, \Omega_\Lambda)$  is a cosmology- and redshift-dependent overdensity factor. In an Einstein-de Sitter universe,  $\Delta_V \simeq 178$  at all redshifts; for  $\Omega_M < 1$ ,

$\Delta_V$  is larger than this value, and increases with decreasing redshift. Kitayama & Suto (1996) have derived analytic approximations for  $\Delta_V(z)$  as a function of  $\Omega_M$  for flat and open cosmologies, and we use their formulae in this paper.

The definition of virial mass above means that one cannot compute  $M_V$  from observational data, such as velocity dispersion, X-ray temperature, or weak lensing, without specifying both a cosmology ( $\Omega_M$  and  $\Omega_\Lambda$ ) and a model for the radial mass distribution of the cluster. The X-ray or velocity data are usually derived from the dense, central parts of the cluster ( $r \lesssim 500h^{-1}$  kpc), whereas the virial radius is generally in the range  $1\text{--}1.5h^{-1}$  Mpc for massive clusters. Consequently, an extrapolation is entailed. Weak lensing data do yield mass as a function of aperture that, in the case of MS1054, extend nearly to the virial radius, but the mass in question is a projected mass density, so that, again, a model is required to obtain the virial mass. These issues are not always well appreciated; in this section we derive  $M_V$  in the context of a specific mass model in order to make clear the assumptions involved.

We adopt the profile of Navarro, Frenk, & White (1997; NFW), which has been shown to be a good fit to cluster-scale dark matter halos in N-body distributions. The NFW profile has a density distribution given by

$$\rho(r) = \frac{\rho_{crit} \delta_c}{x(1+x)^2}, \quad (21)$$

where  $x \equiv r/r_s$  and  $r_s$  is a scale radius for the halo. The central density is determined by the parameter  $\delta_c$ , which one expects to be of order  $10^4$  for massive clusters. The mass interior to radius  $r$  is then given by

$$M(r) = 4\pi\rho_{crit} \delta_c r_s^3 \left[ \ln(1+x) - \frac{x}{1+x} \right]. \quad (22)$$

Substituting equation 22 into the expression for virial mass yields

$$\frac{\ln(1+x_V) - \frac{x_V}{1+x_V}}{x_V^3} = \frac{\Delta_V(1+z)^3 \Omega_M}{3\delta_c}, \quad (23)$$

where  $x_V \equiv r_V/r_s$ .

#### 4.1. Obtaining $M_V$ from X-ray temperature or velocity dispersion

Now let us suppose that the observational data consist either of a measurement of the X-ray temperature  $T_X$  of the intracluster gas, or of the rms line-of-sight velocity dispersion of cluster galaxies,  $\sigma_v$ . Applying the equation of hydrostatic equilibrium to the former, or the Jeans equation to the latter, leads to the equation

$$\frac{GM(r)}{r^2} \rho_{X,g} = -\frac{d}{dr} (\rho_{X,g} u^2), \quad (24)$$

where  $\rho_{X,g}$  is the density of the X-ray emitting gas or the galaxy population at radius  $r$ , and

$$u^2 = \begin{cases} \frac{kT_X}{\mu m_p}, & \text{X-ray gas;} \\ \sigma_v^2, & \text{galaxy velocities.} \end{cases} \quad (25)$$

We can solve equation 24 if we make the simplifying assumption that the tracer (gas or galaxies) distribution

is roughly isothermal at the radii from which most of the X-ray emission (galaxy velocities) are derived,  $r \approx r_s$ . I.e., we assume that  $d \ln \rho_{X,gas} / d \ln r \approx -2$ ,  $u^2 \approx \text{constant}$ . This assumption is reasonable if the gas (galaxies) approximately trace the dark matter potential, because the NFW profile itself is nearly isothermal at such radii. With the isothermal assumption we obtain from equation 24 the relation

$$\delta_c \approx 7 \left( \frac{u}{H_0 r_s} \right)^2. \quad (26)$$

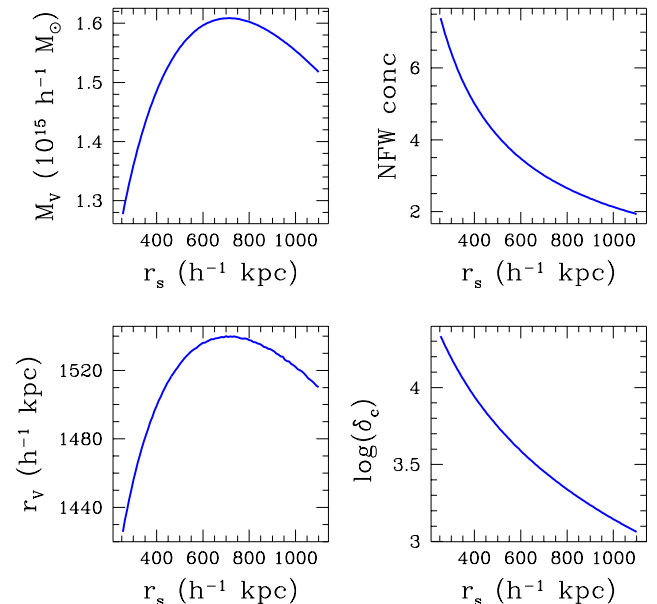


FIG. 4.— The virial mass (upper left panel), virial radius (lower left panel), NFW concentration parameter (upper right panel), and dimensionless central density  $\delta_c$  (lower right panel), for a cluster with an X-ray temperature of 12.3 keV, plotted as a function of the adopted value of the NFW scale radius  $r_s$ . See text for details.

Equation 26 shows that  $\delta_c$  is determined from observations (i.e.,  $T_X$  or  $\sigma_v$ ) only if the scale radius  $r_s$  is known. In other words, the two NFW parameters cannot be determined from a single piece of information. Nevertheless, one might hope that the virial mass itself is insensitive to the particular values of  $\delta_c$  and  $r_s$  provided they are related by equation 26. This indeed turns out to be the case, as we show by adopting the following procedure. First, we pick a value of  $r_s$  in the range  $250\text{--}1100h^{-1}$  kpc. From this we derive  $\delta_c$  from equation 26 and insert the result into equation 23 to obtain  $x_V$ . Substituting into equation 22 then yields, after some algebra, the result

$$M_V = \frac{21}{2} \frac{u^2}{G} r_s \left[ \ln(1+x_V) - \frac{x_V}{1+x_V} \right]. \quad (27)$$

Several aspects of equation 27 merit further comment. First,  $x_V$  is a function of the observable  $u$  and the adopted value of  $r_s$ . Thus,  $M_V$  is not quadratic in  $u$  and linear in  $r_s$ . Indeed, the virial mass is virtually independent of the

adopted value of  $r_s$ , as was argued above. This is shown in the upper left panel of Figure 4, in which the  $M_V$  is computed from an X-ray temperature of  $T_X = 12.3$  keV, the value obtained by Donahue *et al.* (1998) for MS1054 (cf. § 5). (The figure assumes a flat,  $\Omega_M = 0.3$  cosmology at  $z = 0.83$ , the redshift of MS1054.) For  $300 \lesssim r_s \lesssim 1000 h^{-1}$  kpc,  $M_V$  varies by less than  $\sim 10\%$  from its mean value of  $1.3 \times 10^{15} h^{-1} M_\odot$  for the adopted  $T_X$ . The virial radius  $r_V$  changes by an even smaller percentage over this range. In contrast, the inferred central density  $\delta_c$  is quite sensitive to the adopted  $r_s$ . To constrain  $r_s$  further, the NFW concentration index  $c$  is plotted in the upper right hand panel. (This quantity is not simply equal to  $r_V/r_s$ , as it is in Navarro *et al.*, because the virial overdensity is not taken to be exactly 200.) For massive clusters, the simulations of Navarro *et al.* suggest that  $c \simeq 3-5$ . Thus, the plausible values of  $r_s$  are in the range  $300 \lesssim r_s \lesssim 700 h^{-1}$  kpc. As we have seen,  $M_V$  varies little for  $r_s$  in this range. Consequently, we can be assured that our procedure introduces less than about 10% error in the virial mass.

Second, the virial mass as determined from equation 27 differs from what would be obtained had we assumed (as is usually done) a purely isothermal structure for the cluster. Specifically, the virial mass obtained from the NFW model is 10–20% *larger* than an isothermal mass estimate, with the precise factor depending on the typical concentration index. In a sense it is reassuring that the difference is relatively small; on the other hand, as we shall see below, even small mass differences can be crucial in terms of inferences about nongaussianity. Constraining the mass profiles of clusters is thus an important ongoing task for cluster physics.

Last, it is important to bear in mind that  $M_V$  as derived from equation 27 is dependent on the adopted cosmology and redshift, via equation 23, from which  $x_V$  is derived. Thus, *the virial mass of a cluster, derived from temperature or velocity observations, cannot be specified independently of adopted cosmology.* This property of the virial mass, as defined by the PS formalism, will be important in the analysis presented below.

#### 4.2. Obtaining $M_V$ from weak lensing data

Weak lensing data constitute the third and, in principle, most rigorous means of deriving cluster masses, as there is no need to assume hydrostatic or dynamical equilibrium. Deriving a virial mass given aperture mass measurements nonetheless requires care, as we now discuss.

The quantity measured directly by a weak lensing shear analysis (e.g., Luppino & Kaiser 1996) is the mean dimensionless surface density  $\bar{\kappa}$  within an angular radius  $\theta$  of the cluster center. The projected mass within  $\theta$  is then given by

$$M(\theta) = \bar{\kappa} \frac{c^2}{4\pi G} \frac{D_S D_L}{D_{LS}} \pi \theta^2, \quad (28)$$

where  $D_L$ ,  $D_S$ , and  $D_{LS}$  are the lens, source, and lens-source angular diameter distances respectively. These angular diameter distances are all cosmology-dependent; moreover, the typical redshift of the lensed sources must be assumed. These factors all influence the derived virial mass. Evaluating numerical factors in equation 28 yields

$$M(\theta) = 2.13 \times 10^{15} \frac{\bar{\kappa}}{0.1} \left(\frac{\theta}{4'}\right)^2 \frac{y_{LYS}}{(1+z_L)y_{LS}} h^{-1} M_\odot, \quad (29)$$

where the  $y$ 's are the dimensionless comoving angular diameter distances as defined by Peebles (1993).

To make the connection with the NFW halo parameters, we must equate the observationally derived aperture mass above with the projected mass calculated from the NFW formulae; we show elsewhere (Willick & Padmanabhan 1999) that this is given by

$$M(\theta; \delta_c, r_s) = 4\pi \rho_{crit} \delta_c r_s^3 \beta(D_L \theta / r_s), \quad (30)$$

where

$$\beta(x) = \int_0^x y dy \int_0^\infty (y^2 + w^2)^{-1/2} (1 + y^2 + w^2)^{-1} dw \quad (31)$$

is the projected (dimensionless) mass density for the NFW profile. (Explicit expressions for  $\beta$  are given by Willick & Padmanabhan 1999.) Equating the lensing-inferred aperture mass (equation 29) with the NFW model aperture mass (equation 30) yields the following expression for  $\delta_c$  as a function of  $r_s$ ,  $\bar{\kappa}$ , and  $\theta$ :

$$\delta_c = 4886 \frac{\bar{\kappa}}{0.1} \left(\frac{\theta}{4'}\right)^2 \beta^{-1} \left(\frac{r_s}{500 \text{ kpc}}\right)^{-3} \frac{y_{LYS}}{(1+z_L)y_{LS}}. \quad (32)$$

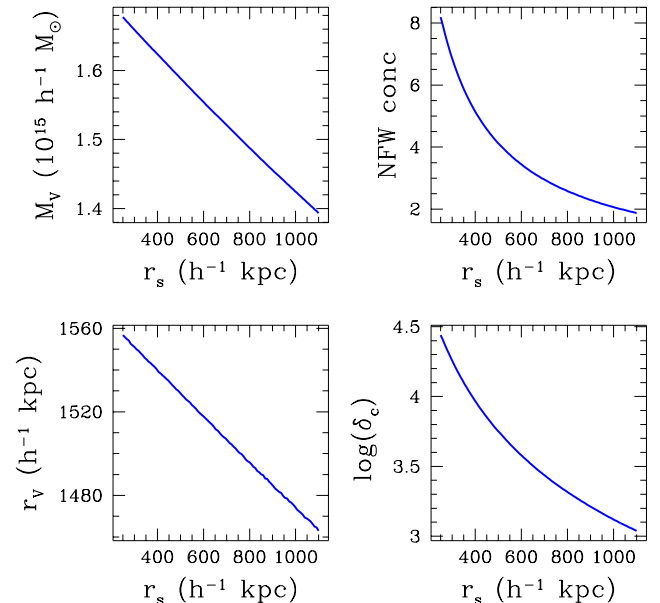


FIG. 5.— Same as the previous figure, except that now the virial mass and related quantities are derived from lensing data. A mean convergence of  $\bar{\kappa} = 0.08$  within  $\theta = 4'$ , the values for MS1054, have been used in the calculation.

Equation 32 is the analogue of equation 26 for the case of a lensing measurement; it gives  $\delta_c$  from the data for any adopted value of  $r_s$ . This suggests that we proceed as above: pick a value of  $r_s$  within a sensible range; calculate the corresponding  $\delta_c$  from equation 32, and thus the virial radius in units of  $r_s$ ,  $x_V$ , from equation 23; obtain the virial mass  $M_V = 4\pi r_V^3 \Delta_V \bar{\rho} / 3$ . We expect that,

as found in the temperature/velocity dispersion case, the virial mass will be insensitive to the choice of  $r_s$ . Figure 5, in which virial mass, radius, NFW concentration index, and central density are plotted for the lensing parameters of MS1054 (see next section), shows that this is once again the case.

### 5. THE VIRIAL MASS OF MS1054

We now apply the methods of the previous section to estimate the virial mass of MS1054 as a function of  $\Omega_M$ . We assume a flat universe,  $\Omega_M + \Omega_\Lambda = 1$ , so that the quantity  $\Delta_V(z)$  discussed in the previous section is fully determined by  $\Omega_M$ .

MS1054 lies at a redshift of  $z = 0.833$  (Tran *et al.* 1999, T99), making it one of the most distant confirmed rich clusters. Its mass can be estimated via each of the three principal methods of the previous section. T99 found it to have a velocity dispersion of  $1170 \pm 150 \text{ km s}^{-1}$  based on 24 galaxies. An earlier determination of the velocity dispersion by Donahue *et al.* (1998; D98) found  $\sigma_v = 1360 \text{ km s}^{-1}$  based on 12 galaxies. D98 also obtained ASCA data for MS1054, from which they deduced a temperature of  $T_X = 12.3^{+3.1}_{-2.2} \text{ keV}$  for the intracluster gas, equivalent to a velocity dispersion  $kT_X/\mu m_p = (1413 \text{ km s}^{-1})^2$  for  $\mu = 0.59$ , the value adopted by Borgani *et al.* (1999). Luppino & Kaiser (1997, LK97) obtained  $V$  and  $I$  band images of MS1054 at the 2.2 m telescope on Mauna Kea in good ( $\sim 1''$ ) seeing, and used these data to estimate  $\bar{\kappa}(\theta)$ . Their mass estimates (for which they assumed  $\Omega_M = 1$ ) indicate a  $\bar{\kappa} = 0.1$  for  $\theta = 4$  arcmin. However, a more conservative estimate, obtained from their Figure 7, is  $\bar{\kappa} = 0.08$  for  $\theta = 4'$ , and we use this more conservative estimate here.

Using these data we can determine the virial mass of MS1054 for an adopted cosmology. Because of the  $\sim 10\%$  variations in the deduced mass with the adopted value of  $r_s$ , we must impose an additional constraint. The most reasonable one to adopt is to require the NFW concentration parameter  $c$  to take on a particular value. Here we choose  $c = 4$ . For the lensing mass, an additional assumption is required, namely, the mean redshift,  $z_S$ , of the lensed galaxy population. Here we choose  $z_S = 1.5$ , which LK97 considered the most suitable value, and which yields mass estimates midway between the minimum ( $z_S \approx 1$ ) and maximum ( $z_S \approx 3$ ) allowed values (LK97).

Figure 6 shows the virial masses obtained via each of the three methods as a function of  $\Omega_M$ . The cosmological dependence of the virial mass is clear. We have also calculated, for use in the next section, a weighted average mass and the  $1\sigma$  errors on this average. Mass errors were estimated by considering the principal sources of error for each method: velocity dispersion uncertainty for the dynamical mass, temperature uncertainty for the X-ray mass, and source redshift uncertainty for the weak lensing mass. The corresponding mass errors were estimated to be 42%, 35%, and 40% respectively. The individual masses were weighted inversely with the squares of the fractional mass errors to obtain the average mass, which is shown as a heavy solid curve in the plot; the shaded region around the average shows its  $\pm 1\sigma$  uncertainty, which is  $\sim 22\%$ .

As the figure shows, while the X-ray and lensing masses agree to within  $\sim 10\%$  for  $\Omega_M \lesssim 0.5$ , the dynamical mass is 40–50% smaller than the other two. This difference is

within the observational errors, and thus is not indicative of systematic differences. Nonetheless, the sensitivity of the PS-predicted cluster abundance to mass makes this difference potentially significant. We discuss this important issue further in § 7.2

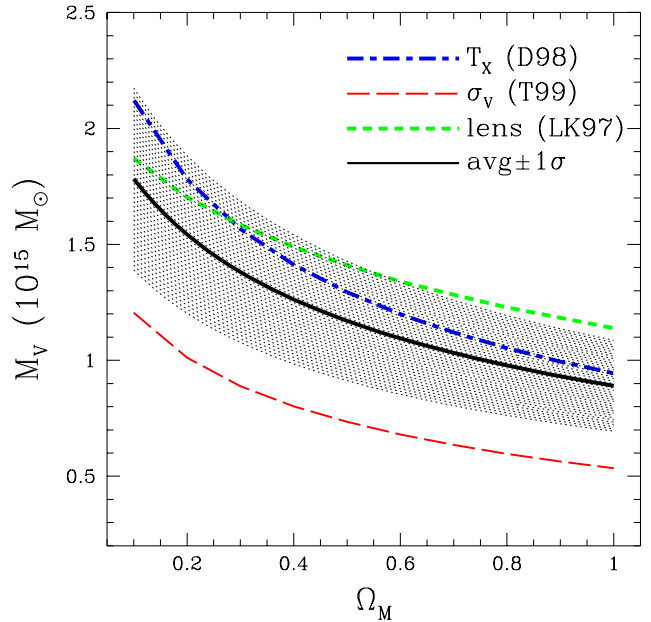


FIG. 6.— The virial mass of MS1054 computed from X-ray, galaxy velocity, and lensing data, plotted as a function of  $\Omega_M$ . The weighted average is plotted as a solid black line, with the light shading showing the  $\pm 1\sigma$  errors.

### 6. METHOD OF ANALYSIS AND BASIC RESULTS

In order to apply the PS formalism to high-redshift clusters, one must first normalize the mass fluctuations on cluster scales by requiring the PS prediction to match observations at *low* redshift. The result is generally expressed as a relationship between  $\sigma_8$ , the value of  $\sigma_M$  within a top-hat sphere of radius  $8h^{-1} \text{ Mpc}$ , and  $\Omega_M$ . Recent results obtained from X-ray temperature and luminosity data include those of Borgani *et al.* (1999):

$$\sigma_8 = (0.58 \pm 0.06) \times \Omega_M^{-0.47+0.16\Omega_M}; \quad (33)$$

Wang & Steinhardt (1998):

$$\sigma_8 = (0.50 \pm 0.10) \times \Omega_M^{-0.43-0.33\Omega_M}; \quad (34)$$

and Pen (1998):

$$\sigma_8 = (0.53 \pm 0.05) \times \Omega_M^{-0.53}. \quad (35)$$

(In each case, results for a flat universe,  $\Omega_M + \Omega_\Lambda = 1$ , are given; in the case of Wang & Steinhardt (1998) nominal values of other cosmological parameters have been adopted. See the original papers for further details.) Similar expressions have been given by Eke, Cole, & Frenk (1996), Girardi *et al.* (1998), and Suto *et al.* (1999).

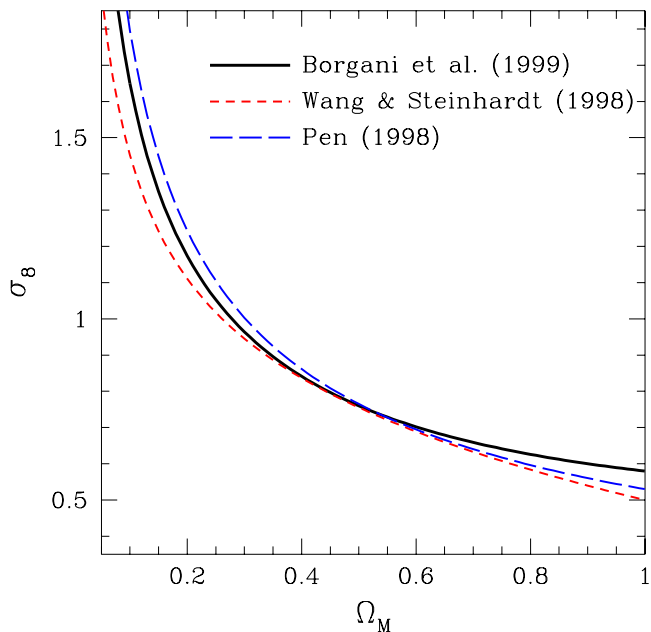


FIG. 7.— Three recently published  $\sigma_8$ - $\Omega_M$  relations derived from low-redshift cluster X-ray temperature and luminosity data.

Figure 7 shows  $\sigma_8$  as a function of  $\Omega_M$  as given by equations 33, 34, and 35. The agreement is within the reported errors, and is especially good for  $0.4 \lesssim \Omega_M \lesssim 0.7$ . However, because of the exponential sensitivity of the PS abundance predictions to  $\sigma_M$ , the small differences in figure 7 have a nonnegligible effect on the inferred degree of nongaussianity. In what follows, we adopt the Borgani *et al.* (1999) calibration, which is intermediate between the other two for  $\Omega_M$  in the observationally preferred range ( $\sim 0.2$ – $0.5$ ). Furthermore, it is based on the most extensive and recent compilation of X-ray data, on which the conclusions of the present paper heavily depend.

### 6.1. Effect of nongaussianity on the $\sigma_8$ - $\Omega_M$ relation

The above low-redshift  $\sigma_8$ - $\Omega_M$  relations were, of course, derived under the assumption of Gaussian primordial density perturbations. If we relax this assumption—e.g., assume the fluctuations are described by the  $\psi_\lambda$  distribution for finite  $\lambda$ —we expect the  $\sigma_8$ - $\Omega_M$  relation to change as well. To obtain the relation for finite  $\lambda$  we first note that the relations essentially represent the requirement that the  $z = 0$  PS abundance prediction, for any  $\Omega_M$ , match the observed abundances at a characteristic rich cluster mass. Specifically, the Borgani *et al.* (1999) calibration yields  $Mn(M) = 4.2 \times 10^{-6} h^{-1} \text{Mpc}^{-3}$  for  $M = 5.95 \times 10^{14} h^{-1} M_\odot$  (i.e., for  $m = 1$ ). By requiring that this condition hold for finite  $\lambda$  as well, we obtain modified  $\sigma_8$ - $\Omega_M$  relations for any desired degree of nongaussianity.

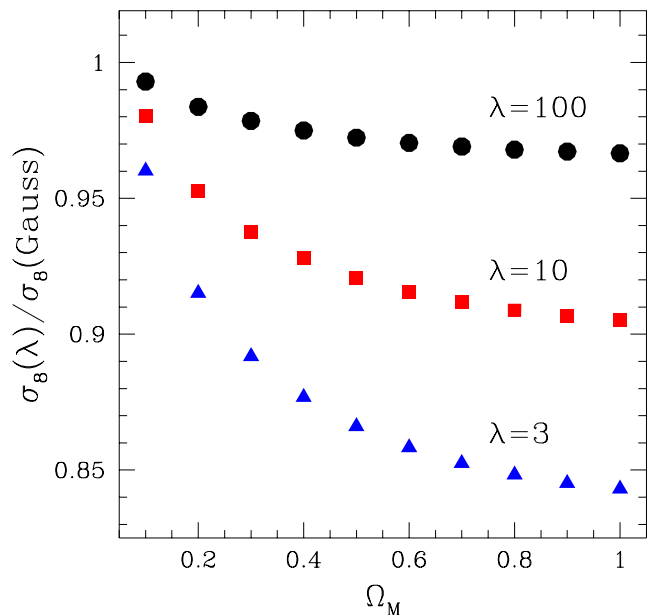


FIG. 8.— The ratio of  $\sigma_8$  for the  $\psi_\lambda$  distribution to the Borgani *et al.* value of  $\sigma_8$ , plotted as a function of  $\Omega_M$ . The values of  $\sigma_8(\lambda)$  were obtained by requiring the generalized PS abundance of  $M = 6 \times 10^{14} h^{-1} M_\odot$  clusters to match that obtained for the Gaussian case, at each value of  $\Omega_M$ .

Figure 8 shows the effect on the  $\sigma_8$ - $\Omega_M$  relation of using the generalized PS abundance formula, equation 13, with the  $\psi_\lambda$  distribution for  $\lambda = 3, 10$ , and  $100$ . It can be seen that the changes relative to the Gaussian case are rather small, especially for  $\Omega_M \leq 0.2$ . This is because low-redshift clusters of moderate mass do not represent very high peaks in the initial density field, for low  $\Omega_M$ . For significant nongaussianity  $\lambda \lesssim 3$  and  $\Omega_M \gtrsim 0.4$ , the fluctuation normalization is more substantially modified.

### 6.2. Calculating the expected number of MS1054-like clusters

Once we have modified the normalization of the density fluctuations  $\sigma_M$  for a given value of  $\lambda$  as described above, we may calculate the predicted comoving number density of clusters above a given mass threshold using equation 14 with  $\psi = \psi_\lambda$ . When Gaussian fluctuations are assumed, we use equation 11. To determine the number of clusters, of mass and redshift as large or larger than that of MS1054, expected in the EMSS sample, we integrate this number density over redshift, multiplying by the appropriate comoving volume element:

$$\mathcal{N}_{exp} = \omega_{1054} \int_{z_1}^{z_{max}} N(\geq m_{1054}, z) \frac{dV}{dz} dz, \quad (36)$$

where:

1.  $m_{1054}$  is the virial mass, in dimensionless units (cf. § 2.2), of MS1054 as determined by the methods of § 4;

2.  $\omega_{1054}$  is the solid angle covered by the Einstein satellite to a limiting X-ray flux fainter than the observed flux of MS1054. From Tables 1 and 2 of Henrey *et al.* (1992) we find  $\omega_{1054} = 0.041$  steradian;
3.  $z_1 = 0.833$  is the redshift of MS1054 (T99);
4.  $z_{max}$  is the maximum redshift out to which a cluster whose X-ray luminosity is equal to that of MS1054 could have been detected by the EMSS. In practice,  $N(\geq m, z)$  is dropping so rapidly with increasing redshift that the result is insensitive to  $z_{max}$  for  $z_{max} \gtrsim 1$ , and we conservatively set  $z_{max} = 1.3$  in the calculations to follow;
5.  $dV/dz$  is the cosmology-dependent comoving volume per unit redshift (e.g., equation 13.61 of Peebles 1993).

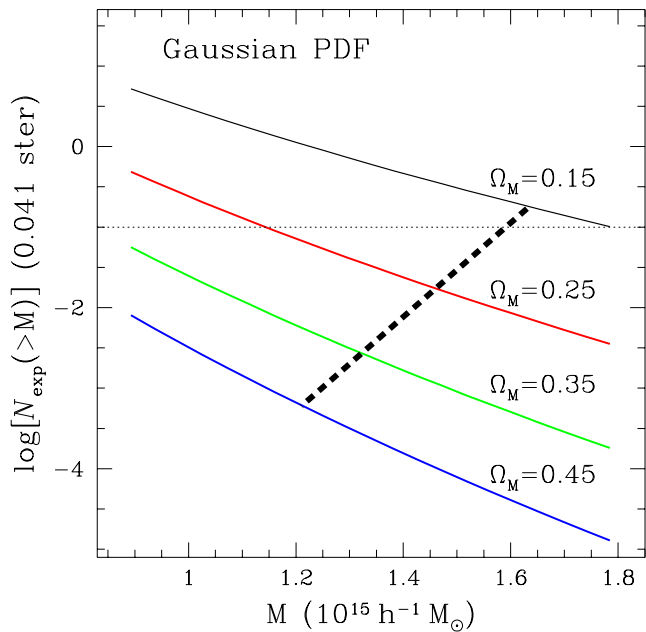


FIG. 9.— Expected number of MS1054-like clusters in the EMSS survey, plotted as a function of mass, under the assumption of Gaussian initial density fluctuations. The  $\sigma_8$ - $\Omega_M$  relation is that of Borgani *et al.* (1999), and a flat universe is assumed. The different curves are for four different values of  $\Omega_M$ . The heavy dashed line sloping down from right to left indicates the variation of the virial mass of MS1054 with  $\Omega_M$  (see Figure 6). The horizontal dotted line indicates a one in ten chance that a cluster as massive as MS1054 would be present in the EMSS survey. Note that only this occurs only for  $\Omega_M = 0.15$ .

Figures 9 and 10 show the results of calculating  $\mathcal{N}_{exp}$  for a Gaussian PDF and a  $\lambda = 1.5$   $\psi_\lambda$ -PDF respectively. Each figure plots  $\mathcal{N}_{exp}$  for four representative values of  $\Omega_M$ . The heavy dashed line sloping down and to the left indicates how the virial mass of MS1054 changes with  $\Omega_M$  (cf. § 5). Where that line intersects the curve for a given  $\Omega_M$  yields the predicted number of MS1054-like clusters in the EMSS. As Figure 9 shows, this number is quite small for all values of  $\Omega_M \geq 0.25$  in the Gaussian case. A cluster at  $z = 0.83$ , and as massive as the lensing, X-ray, and

velocity data for MS1054 indicate that it is, is unlikely to have been found if the fluctuations are Gaussian, unless  $\Omega_M \lesssim 0.2$ .

The situation is significantly changed for a  $\psi_\lambda$ -PDF with  $\lambda = 1.5$ . Figure 10 shows that an MS1054-like cluster now has a better than 10% chance of being found for  $\Omega_M \lesssim 0.4$ . Thus, nongaussian fluctuations allow a much larger value of  $\Omega_M$  to be consistent with the MS1054 data.

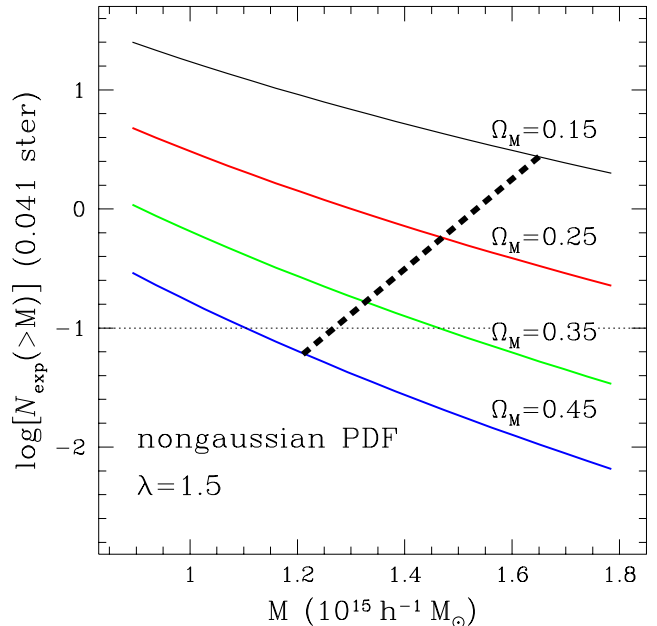


FIG. 10.— Same as the previous figure, except that now the expected number of clusters is calculated using a PDF described by the  $\psi_\lambda$  distribution, with  $\lambda = 1.5$ .

Because we are dealing with a sample of one, we cannot hope to estimate a value of  $\lambda$  per se. It is, however, reasonable to derive an upper limit on  $\lambda$  (i.e., a lower limit on the required degree of nongaussianity) as a function of  $\Omega_M$ . To do so, we calculate, for each  $\Omega_M$ , the value of  $\lambda$  required to yield  $\mathcal{N}_{exp} = 0.1$ , i.e., a one in ten chance that an MS1054-like cluster would be found in the EMSS for that value of  $\Omega_M$ . The resultant value of  $\lambda$  may be thought of as a 90% confidence level upper limit on  $\lambda$ . The corresponding value of the  $T$ -statistic (see Figure 3) would then be a 90% confidence level lower limit.

Figure 11 shows the results of carrying out this calculation, and thus summarizes the main results of this paper. The upper limit on  $\lambda$  decreases from  $\infty$  (Gaussian fluctuations) for  $\Omega_M = 0.17$ , to  $\sim 100$  for  $\Omega_M = 0.20$ , to much smaller values for  $\lambda \gtrsim 0.25$ . As the upper limit on  $\lambda$  decreases with increasing  $\Omega_M$ , signifying increasing nongaussianity, the lower limit on  $T$  increases, from 1 (Gaussian fluctuations) at  $\Omega_M = 0.17$ , to  $\sim 2$  at  $\Omega_M = 0.25$ , to  $\gtrsim 6$  for  $\Omega_M \geq 0.4$ . The required amount of nongaussianity rapidly increases with increasing  $\Omega_M$ . This is ultimately a reflection of the later “freeze-out” time for fluctuation growth in higher density universes.

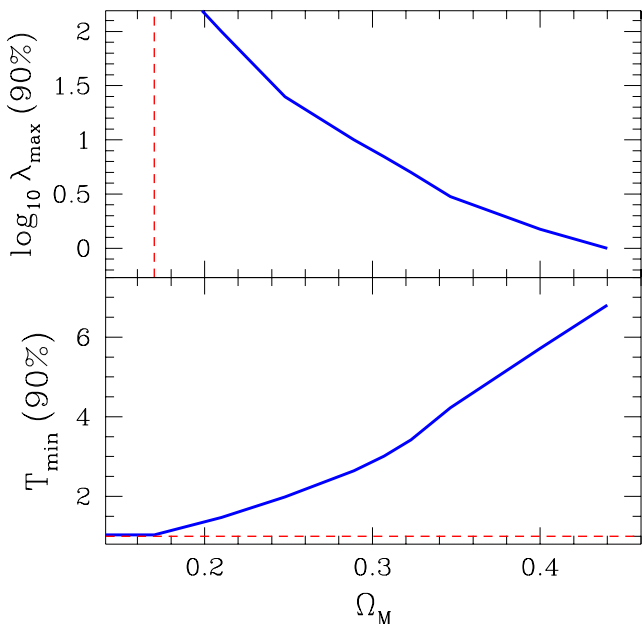


FIG. 11.— The upper panel shows the 90% confidence level upper bound on  $\lambda$  as a function of  $\Omega_M$ . The lower panel shows the corresponding lower bound on  $T$ . These 90% bounds correspond to the amount of nongaussianity required for the expected number of MS1054-like clusters in the EMSS to be  $\geq 0.1$ . See main text for further details.

## 7. DISCUSSION

We have shown that the X-ray selected cluster MS1054–03, at  $z = 0.83$ , adds to a small but growing body of evidence that the primordial density fluctuation field may be nongaussian. Specifically, the high mass of MS1054,  $\gtrsim 10^{15} h^{-1} M_\odot$ , indicates that rare fluctuations,  $\delta/\sigma_M \geq 3$ , are more probable at early times than they would be in the Gaussian case, if  $\Omega_M \gtrsim 0.2$ . In this concluding section, we further discuss several aspects of this result.

### 7.1. Comparison with previous work

#### 7.1.1. Previous analyses based on MS1054

Two other recent papers have considered the cosmological implications of MS1054: D98 (cf. § 5) and Bahcall & Fan (1998; BF98). Both papers reached the conclusion that, by virtue of its high mass, MS1054 by itself rules out an Einstein-de Sitter universe at a high confidence level. D98 stated that MS1054 is consistent with a flat  $\Omega_M = 0.3$  cosmology, while BF98 found that MS1054 is most consistent with  $\Omega_M = 0.2$ . Our results are in rough accord with theirs, although for Gaussian fluctuations we find  $\Omega_M \leq 0.17$ , somewhat smaller than BF98 and markedly lower than D98. The latter difference may result from D98’s conservative estimate of the virial mass of MS1054,  $\sim 7 \times 10^{14} h^{-1} M_\odot$ , which assumed  $\Omega_M = 1$  and an isothermal mass model. In any case, comparison with D98 and BF98 is imprecise because they did not consider nongaussianity as an additional degree of freedom in the abundance analysis; their constraints on  $\Omega_M$  are valid only if the initial density field is Gaussian.

### 7.1.2. Other cluster analyses allowing nongaussianity

A more direct comparison of our results may be made with the recent papers by Robinson, Gawiser, & Silk (1998; RGS98) and Koyama, Soda, and Taruya (1999; KST99). The main points of those papers were summarized in § 1; here we discuss them further in light of our findings.

RGS98 and KST99 considered not only the cluster abundance, but also the cluster correlation length, using observational constraints on the latter obtained from the APM survey (Croft *et al.* 1997), and compared with the predictions of the generalized PS formalism. While increasingly nongaussian PDFs *increase* the predicted cluster abundance (for given  $\Omega_M$  and  $\sigma_8$ ), they *decrease* the predicted correlation length. This helps break the degeneracy between  $\Omega_M$  and nongaussianity (e.g.,  $T$ ) present in any analysis which, like the present one, considers only abundance data. In particular, while our analysis allows Gaussian fluctuations for sufficiently low  $\Omega_M$ , RGS98 and KST99 found that large  $T$  is in fact required for low ( $\lesssim 0.2$ )  $\Omega_M$  in order to accommodate both abundance and correlation length data.

The analyses of RGS98 and KST99 differed in that only the latter used intermediate-redshift cluster abundance as an observational constraint (each considers  $z \lesssim 0.1$  abundances and correlations). This makes KST99 the more powerful probe of parameter space. While RGS98 found an Einstein-de Sitter universe with a Gaussian PDF to be a good fit to the data, KST99 ruled out  $\Omega_M \geq 0.5$ . They found that the required degree of nongaussianity is a minimum for  $\Omega_M \simeq 0.3$ , at which  $T = 3.8 \pm 1.0$ . From Figure 11 we see that for  $\Omega_M \simeq 0.3$  our study indicates  $T \geq 3$ , consistent with the KST99 result. For a flat  $\Omega_M = 0.3$  universe with  $\Gamma = 0.20$ , RGS98 obtained  $T = 4.0_{-2.0}^{+3.6}$ , consistent with both KST99 and this paper.

### 7.2. On the form of nongaussian PDF

KST99 assumed  $P(\delta|M) \propto \chi_m^2(\delta/\sigma_M)$ , whereas we have taken  $P(\delta|M) \propto \psi_\lambda(\delta/\sigma_M)$ . The two PDFs differ more in spirit than in practice. The  $\chi_m^2$  distribution has its roots in a physical model, in which the CDM is produced at the end of an inflationary epoch from  $m$  scalar fields which couple quadratically to a Gaussian inflaton field. The  $\psi_\lambda$  distribution, on the other hand, has no particular physical motivation, being simply a mathematical transformation of the familiar Poisson distribution (§ 3). As we showed in § 3, the two distributions are remarkably similar in terms of their  $T$ -statistic, provided one makes the identification  $m = 9\lambda$ . In fact,  $\chi_{m=9\lambda}^2(x)$  and  $\psi_\lambda(x)$  are similar (though not identical) at all values of  $x$ , not only in their  $T$  values, for  $\lambda \gtrsim 3$ .

Our reason for introducing the  $\psi_\lambda$  distribution is primarily to make the philosophical point that nongaussianity can be modeled phenomenologically, and that as a result we should be cautious in interpreting our findings as evidence of any particular physical model. Thus, although the cluster data point toward a PDF with  $T \approx 4$ , this does not imply that the quadratically coupled inflationary model with  $m \approx 40$  is correct. Indeed, any theory which invokes such a large number of identical but independent scalar fields is suspect on Occam’s Razor grounds alone. More to the point, any PDF with the indicated level of

nongaussianity—such as the  $\psi_\lambda$  distribution with  $\lambda \simeq 3$ —can account for the cluster data.

Of course, even if the  $\psi_\lambda$  distribution proves able to describe the cluster abundance data, this will not necessarily constitute evidence that it is a good description of the PDF. The cluster data test the positive tail of the PDF, not its shape near the peak, which can only be probed via statistics sensitive to regions of average density. The clustering of galaxies in the mildly nonlinear regime, in which perturbation theory (PT) is valid, may allow such a probe. Frieman & Gaztañaga (1999) have applied PT to the angular 3-point correlation function, and have compared their predictions to the APM data. They are able to rule out a strongly nongaussian PDF, the Peebles  $\chi^2$  density field (cf. § 1), which has  $T = 16.3$ , via this approach. They did not, however, consider the milder levels of nongaussianity ( $T \approx 3$ –4) indicated by the cluster data for  $\Omega_M \simeq 0.3$ . Inspection of Figure 1 shows that at such levels ( $\lambda \sim 5$ ) the PDF is close to Gaussian near its peak; it may be quite difficult for the approach of Frieman & Gaztañaga to constrain nongaussianity at this level. Another test of the PDF will be provided by CMB anisotropy data. As mentioned at the outset of the paper, analyses of the COBE data have unearthed indications of nongaussianity. However, those results correspond to a comoving scale of  $\sim 1000h^{-1}$  Mpc, much larger than the  $\sim 10h^{-1}$  Mpc cluster scales probed by clusters. Future CMB measurements sensitive to  $\lesssim 10'$  scale anisotropies will probe cluster mass scales directly. It is not yet clear, however, that the signal-to-noise ratio per resolution element will be sufficient to detect mild nongaussianity. It may well be that for the foreseeable future the cluster data sets will provide the most sensitive tests of PDF nongaussianity.

### 7.3. What does it mean?

If future tests confirm that the initial density field is moderately nongaussian, what would this tell us about the early universe? It was argued above that this would not in and of itself lend credence to any particular inflationary model. Rather, the basic significance of such a finding would be that the fundamental mechanism leading to real-space Gaussianity of the initial fluctuations—their origin as superpositions of numerous, statistically independent individual Fourier modes (equation 1)—is not fully operative. This could be because either (i) only a small number of Fourier modes contribute effectively to  $\delta(\mathbf{x})$ , and the mode amplitudes are themselves nongaussian; (ii) the various Fourier modes are not statistically independent; or (iii) some combination of (i) and (ii). It is the second of these effects which is responsible for nongaussianity in Peebles’ (1999a,b) model, but the first cannot be excluded. Only as observational constraints on nongaussianity improve will be able to construct realistic models of how it arises. This may lead us to a deeper understanding of the fluctuations themselves. Indeed, perhaps the greatest lesson to be learned from this paper and the literature cited herein is that we still know relatively little about the true origin and character of the primordial density fluctuations.

### 7.4. Reasons for Caution

As seen in Figures 9 and 10, the PS-predicted comoving density  $N(\geq M, z)$  is a rapidly decreasing function of mass

for  $M \gtrsim 10^{15} h^{-1} M_\odot$ . Consequently, the predicted number of MS1054-like clusters is extraordinarily sensitive to the mass we assign to MS1054. We have selected this cluster because three high-quality data sets, LK97, D98, and T99, enable us to estimate its mass by three independent methods. However, Figure 6 shows that the velocity dispersion mass estimate for MS1054 is about 50% below the X-ray and lensing estimates. This discrepancy is within the observational uncertainties and thus does not suggest the presence of major systematic errors. On the other hand, if the velocity dispersion mass estimate of T99 is correct, our conclusions would be markedly changed. We would in that case find, using the same criteria as above, that Gaussian fluctuations are allowed for  $\Omega_M \leq 0.33$  as compared with  $\Omega_M \leq 0.17$ , and that for  $\Omega_M = 0.45$  the 90% constraint is  $\lambda \leq 25$  ( $T \geq 2$ ) as compared with  $\lambda \leq 1$  ( $T \geq 7$ ). In short, our conclusion that substantial nongaussianity is indicated by MS1054 is correct only if the X-ray and lensing mass estimates are closer to the truth than the dynamical one.

This extreme sensitivity to mass is both the strength and weakness of the PS approach. It is a strength because it enables even one high-redshift, high-mass cluster such as MS1054 to powerfully constrain cosmology. It is a weakness because it means that even modest random errors in mass estimation drastically affect our quantitative conclusions. To best utilize the PS approach as a cosmological probe, we will need much larger high-redshift ( $z \gtrsim 0.6$ ) cluster samples than are presently available. Each sample cluster will need to have its mass as accurately and robustly measured as MS1054. Only then will the effect of mass errors be reduced, by  $\sqrt{N}$  statistics, to levels at which nongaussianity can be constrained (as a function of  $\Omega_M$ ) with high confidence. The EMSS cluster sample has been the major source of known intermediate and high redshift clusters to date, but its sky coverage is too small at the faintest X-ray flux levels to suffice for future work. Future distant cluster samples will most likely be derived from deep optical surveys to which automated cluster-finding algorithms (e.g., Postman *et al.* 1996; Kepner *et al.* 1998) are applied, with cluster candidates followed up with spectroscopy at 8–10 m class telescopes, X-ray satellite observations, and ground- or space-based deep imaging, to obtain dynamical, X-ray temperature, and weak lensing mass estimates respectively.

The second reason for caution is our reliance on the PS formalism, whose validity at high masses is not yet confirmed. It has long been known from N-body simulations that the PS formula overestimates the number of collapsed objects at low masses,  $M \ll M_*$ , where  $M_*$  is the “non-linear mass” at a given epoch defined by  $\sigma_M(M_*) = \delta_c(z)$ . At masses  $M \gtrsim M_*$ , however, N-body studies have found PS abundance predictions to be remarkably accurate (see, e.g., Borgani *et al.* 1999 and references therein). The non-linear mass at the present time is  $\sim 5 \times 10^{13} h^{-1} M_\odot$ , so that rich clusters are safely above  $M_*$  and thus expected to be well-described by the PS formalism. However, the PS formula has not been exhaustively tested in the very high-mass ( $M \gtrsim 100M_*$ ) regime, for the simple reason that most N-body simulations contain very few objects in this mass range.

With the recent advent of extremely large simulations,

such tests have become possible. In a set of simulations of cubic volumes  $\sim 500h^{-1}$  Mpc on a side, each containing hundreds of rich clusters, Governato *et al.* (1998) were able to test the accuracy of the PS abundance formula for virial masses up to  $\sim 3 \times 10^{15} h^{-1} M_{\odot}$ . They found excellent agreement between the predicted and observed number of clusters in simulations of open,  $\Omega_M = 0.3$ – $0.4$  universes. However, in their  $\Omega_M = 1$  simulation with a low present-day normalization ( $\sigma_8 \lesssim 0.5$ ), they found that the PS formula underpredicted the number of clusters by a factor of  $\sim 3$ – $10$  for masses greater than  $\sim 10^{15} h^{-1} M_{\odot}$ .

The case for which Governato *et al.* found PS to be inaccurate,  $\Omega_M = 1$ , is not one that is relevant to this paper (we considered only  $\Omega_M \leq 0.5$ ), and for low-density universes (the case of interest here) Governato *et al.* confirmed the PS abundance predictions. Still, these results are cause for concern, because if PS underpredicts abundances, we may be led to spurious evidence for nongaussianity. On balance, then, while the present evidence from N-body simulations favors continued use of the PS formalism for cluster analysis, the Governato *et al.* findings suggest that continued testing with larger simulations is needed.

### 7.5. Conclusion

We have used the generalized PS formalism to calculate the likelihood that a cluster as massive as MS1054–03, at a redshift of  $z = 0.83$ , would have been found in the EMSS sample. The calculations assumed a flat universe,  $\Omega_M + \Omega_{\Lambda} = 1$ , and mass fluctuations  $\sigma_M$  normalized to the observed abundance of low-redshift ( $z \leq 0.1$ ) clusters. The expected number of MS1054-like clusters then depends on  $\Omega_M$  and the deviations from Gaussianity of the PDF,  $P(\delta|M)$ , on cluster mass scales. We characterized departures from Gaussianity by assuming  $P(\delta|M) = \sigma_M^{-1} \psi_{\lambda}(\delta/M)$ , where  $\psi_{\lambda}(x)$  is defined by equation 16. The parameter  $\lambda$  quantifies the degree of nongaussianity;  $\psi_{\lambda}$  approaches Gaussianity for  $\lambda \gg 1$ .

Special attention has been given to the problem of estimating cluster virial masses from galaxy velocity, X-ray temperature, and weak lensing data. Such estimates are dependent on the assumed density profile of the cluster, for which we have adopted the NFW form, which has been shown in N-body simulations to be more realistic than any pure power law. We elected to work with MS1054 alone because quality X-ray temperature, galaxy velocity, and lensing data have been obtained for it (D98, T99, LK97), making it a uniquely well-studied high-redshift cluster at this time. The X-ray and lensing mass estimates are in excellent agreement; the dynamical mass is  $\sim 50\%$  smaller than the other two, but this is within the observational errors.

If the initial density fluctuations are Gaussian, it is improbable that a cluster of the mass, redshift, and X-ray flux of MS1054 would be found in the EMSS if  $\Omega_M \geq 0.2$ . For example, the chances of finding an MS1054-like cluster, for a Gaussian PDF, in the EMSS search volume is less than about one in fifty if  $\Omega_M = 0.25$ , and less than one in three hundred if  $\Omega_M = 0.35$ , as shown in Figure 9. If the PDF is nongaussian, however, the likelihood can be greatly enhanced. To constrain the required amount of nongaussianity, we have determined the value of  $\lambda$  required for an MS1054-like cluster to have a one in ten chance of being found in the EMSS. The results are shown in Fig-

ure 11 as a function of  $\Omega_M$ . The maximum allowed value of  $\lambda$  estimated using this criterion decreases from  $\sim 25$  for  $\Omega_M = 0.25$  to  $\sim 1$  for  $\Omega_M = 0.45$ . These results may also be expressed in terms of the parameter  $T$  (equation 20), which measures the likelihood of  $\geq 3\sigma$  peaks in the density field relative to the Gaussian case. We find  $T \geq 2$  for  $\Omega_M = 0.25$ , increasing to  $T \gtrsim 6$  for  $\Omega_M \gtrsim 0.4$ . In short, for any value of  $\Omega_M \gtrsim 0.25$  the initial density field must be significantly nongaussian, with the extent of nongaussianity increasing rapidly with increasing  $\Omega_M$ .

Because our analysis has considered only the predicted cluster *abundance*, it does not exclude Gaussian fluctuations if we are willing to accept  $\Omega_M < 0.2$ . However, the case for a nongaussian PDF irrespective of  $\Omega_M$  is strengthened if our results are taken in conjunction with those of RGS98 and KST99, who analyzed cluster correlation as well as abundance data. In particular, KST99 found that nongaussianity was required, at the level  $T \simeq 2$ – $6$ , for *all* values of  $\Omega_M$  less than 0.5, and ruled out larger values of  $\Omega_M$ . Our estimate  $T \geq 3$  for  $\Omega_M \geq 0.3$  is consistent with their results. If one takes the findings of RGS98, KST99, and this paper at face value, the case for nongaussian initial density fluctuations is strong indeed.

We have, however, identified two potential weaknesses in our analysis, and by extension with any attempt to constrain cosmological parameters from cluster abundance data. First, the predicted abundances drop precipitously with increasing cluster virial mass at the high masses ( $\gtrsim 10^{15} h^{-1} M_{\odot}$ ) and redshifts ( $\gtrsim 0.5$ ) of interest. This sensitivity translates into large errors in the derived cosmological parameters for even modest ( $\sim 30\%$ ) errors in virial mass. This fundamental problem can only be remedied by much larger catalogs of high-redshift massive clusters; at present, MS1054 is one of but a handful of such objects known. These clusters, once identified, will need to be followed up with X-ray, galaxy velocity, and weak lensing measurements to ensure reliable mass estimates. Efforts are presently under way by this author and collaborators, as well as other groups, to obtain such data sets. In 5–10 years we will undoubtedly know much more than we do now about the evolution of the cluster abundance at  $z \sim 1$ .

The second problem concerns the validity of the Press-Schechter formalism in the high-mass regime. It has become conventional wisdom in recent years that the PS abundance formula “works much better than it should,” based as it is on a simple, spherical collapse model, and as a result it has been widely and fruitfully used. However, if the PS formula underpredicts the actual abundance of high-mass objects, as at least one study suggests (Governato *et al.* 1998), one would underestimate  $\Omega_M$  (if Gaussian fluctuations are assumed) or overestimate departures from Gaussianity by applying the PS formula to cluster abundance data. A challenge for theory and numerical simulations in the coming years is to rigorously test the PS formula at high masses and, if necessary, replace it with a more accurate semianalytical framework. Such theoretical groundwork will be crucially important if the high-quality cluster data sets of the coming decade are to be fully exploited.

The author gratefully acknowledges the support of NSF grant AST-9617188, the Research Corporation, and a

Frederick Terman Fellowship from Stanford University. The author thanks Nikhil Padmanabhan and Puneet Batra for assistance in developing the Press-Schechter computer codes, and Nikhil Padmanabhan, Puneet Batra,

Keith Thompson, and Sarah Church for useful discussions. Finally, the author would like to thank Joanne Cohn for bringing a number of papers on primordial nongaussianity to his attention.

## REFERENCES

- Bahcall, N.A. 1999, preprint (astro-ph/9901076)  
 Bahcall, N.A., & Fan, X. 1998, ApJ, 504, 1 (BF98)  
 Bardeen, J.M., Bond, J.R., Kaiser, N., & Szalay, A.S. 1986, ApJ, 304, 15  
 Bennett, C.L., Banday, A.J., Gorski, K.M., Hinshaw, G., Jackson, P.D., Keegstra, P., Kogut, A., Smoot, G.F., Wilkinson, D.T., & Wright, E.L. 1996, ApJ, 464, 1  
 Borgani, S., Rosati, P., Tozzi, P., & Norman, C. 1999, preprint (astro-ph/9901017)  
 Bromley, B.C., & Tegmark, M. 1999, preprint (astro-ph/9904254)  
 Bunn, E.F., & White, M. 1997, ApJ, 480, 6  
 Croft, R.A.C., Dalton, G.B., Efstathiou, G., Sutherland, W.J., & Maddox, S.J. 1997, MNRAS, 291, 305  
 Donahue, M., Voit, G.D., Gioia, I., Luppino, G., Hughes, J.P., & Stocke, J.T. 1998, ApJ, 502, 557 (D98)  
 Eke, V.R., Cole, S., & Frenk, C.S. 1996, MNRAS, 282, 263  
 Ferreira, P.G., Gorski, K.M., & Magueijo, J. 1998, ApJ, 503, L1  
 Ferreira, P.G., Gorski, K.M., & Magueijo, J. 1999, preprint (astro-ph/9904073)  
 Frieman, J.A., & Gaztañaga, E. 1999, preprint (astro-ph/9903423)  
 Gaztañaga, E., Fosalba, P., & Elizalde, E. 1998, MNRAS, 295, 35  
 Girardi, M., Borgani, S., Giurcin, G., Mardrossian, F., & Mezzetti, M. 1998, ApJ, 506, 45  
 Gorski, K.M., Banday, A.J., Bennett, C.L., Hinshaw, G., Kogut, A., Smoot, G.F., & Wright, E.L. 1996, ApJ, 464, L11  
 Governato, F., Babul, A., Quinn, T., Tozzi, P., Bauch, C.M., Katz, N., & Lake, G. 1998, preprint (astro-ph/9810189)  
 Henry, J.P., Gioia, I.M., Maccacaro, T., Morris, S.L., Stocke, J.T., & Wolter, A. 1992, ApJ, 408, 419  
 Kepner, J., Fan, X., Bahcall, N., Gunn, J., Lupton, R., & Xu, G. 1998, preprint (astro-ph/9803125)  
 Kitayama, T., & Suto, Y. 1996, ApJ, 480, 493  
 Koyama, K., Soda, J., & Taruya, A. 1999, preprint (astro-ph/9903027) (KST99)  
 Liddle, A.R., Lyth, D.H., Schaefer, R.H., Shafi, Q., & Viana, P.T.P. 1996, MNRAS, 281, 531  
 Luppino, G.A., & Kaiser, N. 1997, ApJ, 475, 20 (LK97)  
 Magueijo, J., Ferreira, P.G., & Gorski, K.M. 1999, preprint (astro-ph/9903051)  
 Martin, J., Riazuelo, A., & Sakellariadou, M. 1999, preprint (astro-ph/9904167)  
 Navarro, J.F., Frenk, C.S., & White, S.D.M. 1997, ApJ, 490, 493 (NFW)  
 Novikov, D., Feldman, H., & Shandarin, S. 1998, preprint (astro-ph/9809238)  
 Pando, J., Valls-Gabaud, D., & Fang, L.-Z. 1998, preprint (astro-ph/9810165)  
 Peebles, P.J.E. 1993, *Physical Cosmology*, (Princeton: Princeton University Press)  
 Peebles, P.J.E. 1999a, ApJ, 510, 523  
 Peebles, P.J.E. 1999b, ApJ, 510, 531  
 Pen, U.-L. 1998, ApJ, 498, 60  
 Postman, M., Lubin, L.M., Gunn, J.E., Oke, J.B., Hoessel, J.G., Schneider, D.P., & Christensen, J.A. 1996, AJ, 111, 615  
 Press, W.H., & Schechter, P. 1974, ApJ, 187, 425 (PS)  
 Robinson, J., Gawiser, E., & Silk, J. 1998, preprint (astro-ph/9805181) (RGS98)  
 Salopek, D.S. 1999, preprint (astro-ph/9903327)  
 Suto, Y. *et al.* 1999, preprint (astro-ph/9902350)  
 Tran, K.-V. H., Kelson, D.D., van Dokkum, P., Franx, M., Illingworth, G.D., & Magee, D. 1999, preprint (astro-ph/9902349) (T99)  
 Wang, L., & Steinhardt, P.J. 1998, preprint (astro-ph/9804015)  
 Wang, L., Caldwell, R.R., Ostriker, J.P., & Steinhardt, P.J. 1999, preprint (astro-ph/9901388)  
 White, M. 1998, preprint (astro-ph/9811227)  
 Willick, J., & Padmanabhan, N. 1999, in preparation

## APPENDIX

APPROXIMATING  $\sigma_M(R)$ 

In this appendix we obtain an approximation for  $\sigma_M(R)$  that is valid for CDM models. Using equations 5 and 6 in the main text, and assuming for simplicity  $n = 1$ , we may write the mass variance as follows:

$$\sigma_M^2(R) = \delta_H^2 \left( \frac{c}{H_0 R} \right)^4 \mathcal{I}(\Gamma R), \quad (\text{A1})$$

where

$$\mathcal{I}(\Gamma R) \equiv \int_0^\infty x^3 W^2(x) T^2 \left( \frac{x}{\Gamma R} \right) dx. \quad (\text{A2})$$

Equation A1 further simplifies to

$$\ln \sigma_M(R) = 16.012 + \ln \delta_H + 0.5 \ln \mathcal{I}(\Gamma R) - 2 \ln R, \quad (\text{A3})$$

when  $R$  is given in  $h^{-1}$  Mpc.

Equation A3 shows that  $\sigma_M(R)$  is fully determined, apart from a normalizing constant involving  $\delta_H$ , by  $\ln \mathcal{I}(\Gamma R)$ . Since we fix the normalization by the cluster abundance at low redshift, the  $\delta_H$  term is unimportant here, and a suitable expression for  $\mathcal{I}(\Gamma R)$  is *all* we need to evaluate  $\sigma_M(R)$ . We have obtained such an expression by numerically evaluating  $\mathcal{I}(\Gamma R)$  for a range  $\Gamma R$  and fitting the results to a low-order polynomial of the form

$$\ln \mathcal{I}(\Gamma R) = \sum_{n=0}^m a_n [\ln(\Gamma R)]^n. \quad (\text{A4})$$

Choosing  $m = 5$  produced a fit with better than 0.1% accuracy for  $1 \leq \Gamma R \leq 8$ , fully covering the range of expected values. In Table A1 we give the coefficients yielding the best fifth-order fit. Substituting this polynomial expression into equation A3 yields  $\sigma_M$  up to a normalizing coefficient. The expression for the logarithmic derivative of  $\sigma_M$  needed for the PS abundance formula is then simply

$$\frac{d \ln \sigma_M}{d \ln R} = \frac{1}{2} \sum_{n=1}^m n a_n [\ln(\Gamma R)]^{n-1} - 2. \quad (\text{A5})$$

TABLE A1

Fit Coefficients for Computing  $\ln \mathcal{I}(\Gamma R)$ 

$a_0$	$a_1$	$a_2$	$a_3$	$a_4$	$a_5$
-4.7783	2.7251	-0.1811	-0.0232	-0.0053	0.0014

Notes: Coefficients in the expansion defined by equation A4.